Title
Diffusion tensor imaging correlates of depressive symptoms in Parkinson disease

Journal
The Journal of Comparative Neurology, 530(10)

ISSN
1550-7149

Authors
Uhr, Lauren
Tsolaki, Evangelia
Pouratian, Nader

Publication Date
2022-07-01

DOI
10.1002/cne.25310

Peer reviewed

HHS Public Access

Author manuscript

J Comp Neurol. Author manuscript; available in PMC 2023 July 01.

Published in final edited form as:

J Comp Neurol. 2022 July ; 530(10): 1729–1738. doi:10.1002/cne.25310.

Diffusion tensor imaging correlates of depressive symptoms in Parkinson disease

Lauren Uhr, MPH[1], **Evangelia Tsolaki, PhD**[1], **Nader Pouratian, MD, PhD**[2,*]

[1]Department of Neurosurgery, David Geffen School of Medicine at UCLA, Los Angeles, California

[2]Department of Neurological Surgery, UT Southwestern Medical Center, Dallas, Texas

Abstract

Introduction: Depression is a heterogeneous clinical syndrome prevalent in patients with Parkinson disease (PD) that remains incompletely understood. Further, the differences in biomarkers of depression in PD and in non-PD patients are unclear. The subcallosal cingulate cortex (SCC) and its connections has been implicated in the pathophysiology of major depressive disorder (MDD). Diffusion tensor imaging (DTI) provides a tool to quantify MDD-related structural abnormalities underlying depressive symptoms in PD.

Methods: Diffusion-weighted magnetic resonance imaging data were collected from thirty-one patients with PD. Depression symptom severity was measured using the Beck Depression Inventory (BDI-II), and assessed using three subscales: dysphoric mood, loss of interest/pleasure, and somatic symptoms. Probabilistic tractography methods were used to quantify the SCC connectivity to target regions in cortico-limbic-striatal network (ventral striatum (VS), medial prefrontal cortex (mPFC), dorsal anterior cingulate cortex (ACC), and uncinate fasciculus (UCF)) while fractional anisotropy (FA) was calculated in predefined white matter regions of interest. DTI data was correlated with severity of depression across three domains.

Results: SCC-mPFC connectivity in the left hemisphere was positively correlated with severity of dysphoric mood (Benjamini-Hochberg adjusted $p = 0.02$). ROI-based analyses demonstrated a significant and distinct topographic association between FA and dysphoric mood, loss of interest/pleasure, and somatic symptom severity, although these findings did not maintain significance after applying the false discovery rate correction.

Conclusion: Abnormal SCC connectivity underlies depressive symptoms in both PD and MDD, suggesting that interventions used for MDD should be explored in treating depressive symptoms in PD, particularly depression dominated by dysphoric mood.

Graphical Abstract

*Corresponding Author: nader.pouratian@utsouthwestern.edu, 5323 Harry Hines Blvd, Dallas, TX 75390.

Conflict of interest disclosure: NP is a consultant for Abbott Laboratories, Boston Scientific, Second Sight Medical Products, and Sensoria Therapeutics.

Ethics approval statement: This study was done with approval from the UCLA Institutional Review Board.

Patient consent statement: This retrospective study was conducted with IRB approved waiver of consent.

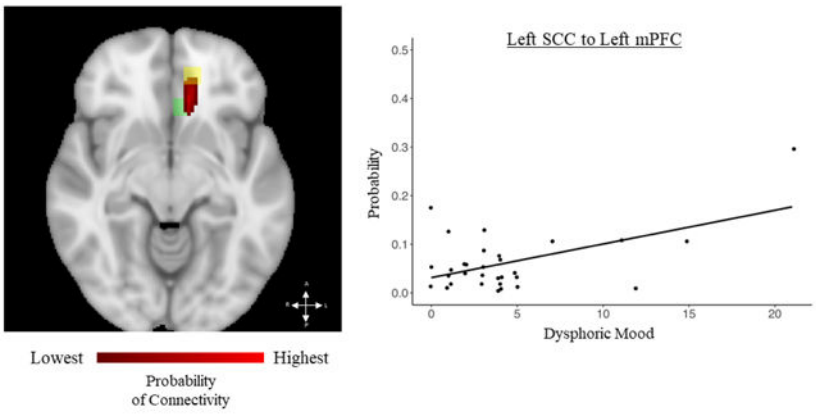

Keywords

Parkinson disease; depression; diffusion; subcallosal cingulate; medial prefrontal cortex

1. Introduction

Parkinson disease (PD) is associated with multiple non-motor symptoms, including depression which is one of the most common non-motor symptoms affecting 40–50% of PD patients [1]. Beyond the emotional disturbances, untreated depression negatively influences patients' quality of life, physical disability, and cognitive dysfunction [1]. Depressive symptoms are thought to be associated with the underlying neurodegenerative disease itself as depression often precedes motor symptoms [1]. Recently, advanced neuroimaging has provided some insights into the neurobiological process of depression in this population. However, the neural substrates and mechanism of disease remain incompletely understood. Studies have used molecular imaging to explore the role of neurotransmitter systems, while other studies have examined the functional or structural connectivity of key brain regions, including the bilateral thalamus, bilateral anterior cingulate, and white matter tracts of the left frontal region [2,3,4]. However, the results have been inconsistent.

Diffusion tensor imaging (DTI) is a noninvasive imaging modality used to characterize the integrity of white matter tracts and the projections of fiber pathways within the brain. Fractional anisotropy (FA), the most common DTI scalar, is believed to reflect white matter microstructure including myelination, packing density, and membrane permeability [5]. DTI has been widely used in connectivity analyses to examine structural underpinnings of motor and behavioral symptoms in PD [6] as well as depression in patients with major depressive disorder (MDD) [7]. Although DTI has provided key insight to the pathology of these two conditions separately, only a few studies have used DTI to examine depression in PD.

The subcallosal cingulate cortex (SCC) and its structural connectivity has been identified as a critical network in the pathophysiology of mood disorders, specifically depression [8]. The SCC is a limbic brain region with extensive connections, forming the limbic-cortical network that processes sadness and regulates emotion [8]. SCC functional and structural connectivity has been correlated with clinical features and treatment outcomes in MDD

[9,10]. Further, the SCC is a target of deep brain stimulation (DBS) for depression, suggesting that stimulation of connections to the ventromedial pre-frontal cortex, nucleus accumbens, and cingulum bundle is related to the therapeutic antidepressant effect [11]. SCC DBS responders compared to non-responders shared activation of the following subject-specific white matter tracts: forceps minor, uncinate fasciculus (UCF), cingulum bundle, and fronto-striatal fibers [12]. Probabilistic tractography, a method that accounts for intra-voxel fiber crossing to quantitatively provide the probability of fiber direction at single voxels, has been used to predict the response to electroconvulsive therapy (ECT) treatment based on the SCC structural connectivity at baseline in MDD patients [10]. Such altered patterns in this limbic-cortical network may be present in depression associated with neurodegenerative diseases such as PD, but has not been explored or characterized.

Region of interest (ROI)-based analyses have been used to compare differences in white matter across individuals. In PD, multiple studies recognize FA changes correlated with motor symptom manifestations [13] and executive dysfunction [14]. To date, more limited evidence suggests that depression in PD is associated with white matter microstructural changes. For example, some studies have found decreased FA in the thalamus bilaterally [4], bilateral anterior cingulate [3], and multiple white matter tracts (left uncinate fasciculus, left superior longitudinal fasciculus, left anterior thalamic radiation, left forceps minor and the inferior longitudinal fasciculus) in the left frontal region in PD patients with depression [2], while another study reported no statistically significant differences [15].

Perhaps, the aforementioned inconsistencies in these findings can be explained by the heterogeneity of the depressive syndrome. In patients with MDD, lower FA has been reported in numerous white matter tracts and most significantly in the corona radiata and corpus callosum [16]. However, recognizing the constellation of MDD clinical features, DTI techniques have been used to examine white matter abnormalities in subtypes of depression. Such depression subtypes can be distinguished by functional connectivity differences within depression-related networks, which are associated with specific clinical symptom profiles [17] and treatment outcome [18]. Therefore, symptom-based research of biomarkers is needed to help understand the pathophysiology of depressive disorders, where subtypes may differentially benefit from therapeutic strategies.

We hypothesize the depressive symptom subscales predict distinct SCC structural connectivity and white matter microstructural changes and these changes would be associated with severity of symptoms. The overall aims of this study include: 1) investigate the relationship between the SCC structural connectivity to the cortico-limbic-striatal circuit using probabilistic tractography and 2) examine the white matter microstructure in predefined ROIs implicated in depression, particularly within the limbic system. The present study is the first to examine the depressive symptomatology in a population with PD and may provide insights into the structural underpinnings of depressive symptoms.

2. Methods

2.1 Subjects

Using UCLA's stereotactic neurosurgery database, this retrospective study included 31 patients (24 males, 7 females, average age of 64.5 ± 5.8 years), who underwent evaluation for stereotactic implantation of deep brain stimulators (DBS) for PD. All patients had preoperative MRI data and comprehensive neuropsychological testing as part of the evaluation for DBS. The patient's mean disease duration was 8.48 ± 3.38 years, with a mean Levodopa equivalent of 1126.33 ± 613.46 mg (range 20–2760). Motor function was measured with the Movement Disorder Society Unified Parkinson's Disease Rating Scale, Part III (UPDRS) (measure in the "off" state). The mean UPDRS score was 35.11 ± 14.09 (range 16–66). This study was done with approval from the UCLA Institutional Review Board.

2.2 Depression Measure

Neuropsychological testing was part of the standard procedure for stereotactic implantation of DBS evaluation. All assessments were completed in an "on" medication state. The Beck Depression Inventory-II (BDI-II), a self-reported 21-item scale measuring the presence and severity of depression symptomatology, was extracted from the neuropsychological assessments. Each item consists of four self-evaluative statements scored 0 to 3. Based on confirmatory factor analysis in a PD population, we used a three-factor model of BDI-II to establish independent scores for three factors of depression: dysphoric mood, loss of interest/pleasure, and somatic symptoms [19]. The summation of the items in each factor was used in the analysis, measuring symptom severity of that factor.

2.3 Imaging Acquisition and Analysis

Each participant underwent MR imaging (Siemens 3T Prisma^{fit}, Erlangen, Germany) using a spin-echo, echo-planar diffusion-weighted single phase encoding direction sequence with 64-directions (matrix=128×128, b value=1000s/mm^2; number of slices=72; 2mm isotropic voxels, repetition time/echo time=7600/66msec) and a high resolution, motion corrected multi-echo MPRAGE T1-weighted sequence (TEs/TR= 2.44/2100ms, TI=1100ms, FA=15°, isotropic 1mm voxels).

Imaging analysis was conducted using Functional Magnetic Resonance Imaging of the Brain (FMRIB) Software Library (FSL) tools [20]. Diffusion and T1 data were stripped of the skull using brain extraction tool (BET). Eddy current correction was performed on each volume in the dataset, applying affine registrations to the initial reference B0 volume. Visual inspection of each DTI data was completed to assess for large artifacts. A multi-fiber diffusion model was fit to each diffusion-weighted imaging. At each voxel, Bayesian techniques were used to estimate the principal diffusion direction, accounting for the possibility of crossing fibers. T1 images were segmented to generate a CSF mask, and subsequently used as an exclusion mask to limit tractography to brain voxels.

2.4 Subject-Specific Regions of Interest

The definition and implementation of subject-specific ROIs (ventral striatum (VS), medial prefrontal cortex (mPFC), dorsal anterior cingulate cortex (ACC), and uncinate fasciculus (UCF)) were adapted from a previous study [10]. The SCC seeds were defined anatomically in MNI152 standard space and then registered into each subject's T1 and diffusion imaging space using linear and non-linear transformations FLIRT-FNIRT. Probabilistic tractography was performed with FDT [21] to characterize the probability of connectivity from the anatomically defined SCC with the whole brain. Tractography was conducted using a whole brain target and CSF exclusion mask with the following parameters: 5000 samples (streamlines), 0.2 curvature threshold, loopcheck termination, 2000 maximum number of steps, 0.5 mm step length and 0.01 subsidiary fiber fraction threshold. The subsequent whole brain tractography map was transformed into MNI152 standard space. The forceps minor, cingulum bundle and fronto-striatal fiber pathways were localized, and their termination area was identified. The anatomical region of each termination area was used to define extended regions of the mPFC, ACC, UCF and VS based on coordinates in MNI152 standard space. Figure 1 illustrates exemplary mPFC and ACC ROIs. For each extended ROI, the voxel with the highest probability of connectivity to SCC was determined and that voxel was used to delineate the center of the subject-specific, connectivity determined target mask (mPFC: 5×5×5 voxel ROI, ACC: 5×5×5 voxel ROI, UCF=2×2×2 voxel ROI and VS: 2×2×2 voxel ROI in MNI152).

2.5 Probabilistic Tractography

To investigate the SCC structural connectivity, FMRIB's Diffusion toolbox was used to perform probabilistic tractography using the same parameters. Using PROBTRACTX, streamlines were generated from each voxel within the seed region and the number of streamlines connecting the seed to each subject-specific target ROI were determined [22]. To guide the tractography to the target ROI from the seed, each ROI target was used as 1) a waypoint mask such that only tracts that pass through the mask will be counted towards the probability of connectivity, 2) a termination mask to stop tracts at the target mask and 3) a classification target to quantitatively estimate the connectivity between each voxel in the seed mask to the target mask. The probability of connectivity for each target ROI was calculated using the following equation, where the number of streamlines from seed to target represent the number of tracts from each voxel in the seed mask to the waypoint target mask, number of seed voxels represent how many voxels were included in the SCC seed mask, and 5000 represent the number of streamlines generated:

$$Probability\,of\,Connectivity = \frac{Number\,of\,strealimes\,from\,seed\,to\,target}{number\,of\,seed\,voxels * 5000}$$

Each subject's SCC tractography map was non-linearly registered to the MNI152 template.

2.6 Diffusion Metrics

Voxel-wise analysis of the FA data was done using Tract-Based Spatial Statistics (TBSS) [23], a part of the FSL toolkit. FA images were generated using FSL's DTIFIT after the aforementioned brain extraction and eddy current correction. The FA images were then

aligned into the FMRIB58_FA standard space using a nonlinearly registration (FNIRT). A mean FA image was then generated and used to create a mean FA skeleton, depicting tracts common to the entire group (FA threshold = 0.2). Each subject's FA map was then projected onto the mean FA skeleton, allowing for an alignment-invariant tract representation.

For the ROI-based analysis, FSL's Johns Hopkins (JHU) DTI-based white-matter atlas was used for automated white matter segmentation, labeling 48 white matter tracts [24] (Table 1). Using fslstats, average FA values were calculated in the 48 ROIs for each subject.

2.7 Data Analysis

Analysis was conducted using SPSS version 26 (IBM Corp. in Armonk, NY). Subjects with missing data were removed prior to analysis. The probability of connectivity from the left and right hemisphere SCC to each target ROIs were linearly regressed against the three model-factor of BDI-II depression symptomatology. In addition, the DTI measure of the 48 ROIs were similarly linearly regressed against the three model-factor of BDI-II depression symptomatology. Further analyses were performed on both models to control for possible confounding by age and sex. We also conducted a sensitivity analysis by including UPDRS in the multivariable models to control for motor function when examining the association of the SCC tracts and/or ROIs with depression symptomatology. To limit the false discovery rate, Benjamini-Hochberg Adjusted *p*-values were calculated with a significance threshold set at $p < 0.05$. The unadjusted relationships that reach a significance threshold of $p < 0.05$ were also reported even if the test was no longer significant after adjustment to delineate trends.

3. Results

Table 2 depicts the demographics of the study population and depressive symptomatology characteristics.

For the probabilistic tractography analysis, the mean SCC connectivity to each ROI was calculated, ranging from 0.001 to 0.567 (Figure 1A). In the univariate analysis examining the relation between the SCC probability of connectivity and depressive symptoms, the probability of connectivity between the SCC in the left hemisphere and the ipsilateral mPFC and ACC was significantly correlated with dysphoric mood ($p = 0.002$) and somatic symptoms ($p = 0.044$), respectively (Figure 2). After controlling for age and sex, the probability of connectivity between the SCC in the left hemisphere and the ipsilateral mPFC and dysphoric mood remained statistically significant ($p = 0.003$) and persisted after the Benjamini-Hochberg *p*-value adjustment ($p = 0.015$). This finding remained statistically significant in the sensitivity analysis adjusting for age, sex and UPDRS score (Table 3A).

The mean FA values for each of the 48 JHU ROIs ranged from 0.125 to 0.806 (Figure 1B). After controlling for age and sex, regression analysis showed significant correlations between ROI FA measures and depression symptomatology in each BDI-II factor: right fornix with dysphoric mood ($p = 0.037$); splenium of the corpus callosum with loss of interest ($p = 0.048$); and ROIs within the limbic system and brainstem with somatic symptoms ($p < 0.041$) (summarized in Table 4). A graphical representation of these

significant ROIs is illustrated in Figure 3. After further controlling for UPDRS score, significant correlations were found between somatic symptoms and the left external capsule, right cingulate gyrus, left superior fronto-occipital fasciculus, and bilateral tapetum (Table 3B). However, these correlations did not retain significance after applying the Benjamini-Hochberg adjustment.

4. Discussion

This study characterizes the DTI changes, specifically the SCC structural connectivity and white matter microstructural correlates, associated with depression symptomatology and severity in patients with PD. Although a few studies have used DTI to better understand depression, apathy and anxiety in PD, none have examined specific symptoms of depression. Overall, our study suggests potentially distinct anatomic subtracts mediating distinct aspects of depression symptomatology in PD, namely dysphoric mood, loss of interest/pleasure, somatic symptom. Most significantly, the ipsilateral SCC probability of connectivity with left mPFC was positively correlated with dysphoric mood. Importantly, the left SCC-mPFC tract remained significant after controlling for motor function, suggesting that these findings are specific to dysphoric mood symptomatology.

The mPFC, connected via bilateral forceps minor of the anterior corpus callosum, is a key node in the limbic-cortical network. The region has been implicated in mood regulation and is thought to regulate the generation of negative emotion [25]. The region's role in emotional and affective function is made clear by a lesion study where individuals with bilateral ventromedial prefrontal cortex lesions have low levels of "cognitive/affective" symptoms such as guilt, self-dislike sadness but normal levels of "somatic" symptoms [26]. This is consistent with our findings as while no statistically significant relationship was found with loss of interest/pleasure and somatic symptoms, dysphoric mood (consisting of the cognitive/affective symptoms) is positively correlated with the probability of connectivity between the SCC and the mPFC in the left hemisphere.

The mPFC has also been implicated in depression in PD. Studies have found abnormalities in blood flow [27] and spontaneous activity [28] in this region in PD patients with depression. Further, repetitive transcranial magnetic stimulation for depression in PD normalized abnormal activity in the prefrontal cortex, more prominently in the left hemisphere [29]. Our findings suggest that increased connectivity between the SCC and mPFC in the left hemisphere is associated with severity of dysphoric mood symptoms. While it was found that differences in structural connectivity between the SCC and mPFC in MDD patients predicted therapeutic outcome to ECT [10], future studies are necessary to investigate whether this is a biomarker for response to therapy in PD.

Previous studies using DTI to study depression in PD have mainly focused on inter-group comparisons between depressed and non-depressed patients with PD. In general, these studies have found decreased FA in the frontal regions and connections to the subcortical-limbic regions in patients with PD and depression [2,3], although the results are inconsistent [15]. Decreased FA values have also been found in the bilateral mediodorsal thalamic regions [4]. When correlating FA values and depression assessment summative scores, a

negative correlation was previously found [2,4]. In the present study, we found a positive trend between FA and all three depression symptoms: dysphoric mood, loss of interest/pleasure, and somatic symptoms. Perhaps, these conflicting findings in PD are due to the heterogeneity of depression symptoms used in these clinical measurements, particularly as different questionnaires are used to assess depression across studies leading to inability for direct comparisons. In MDD patients, increased FA was found in the right ventral tegmental area and differed significantly in a subtype of MDD patients with trait anxiety [30]. Although our findings did not maintain significance when correcting for the false discovery rate, we found evidence of white matter microstructural change in distinct ROIs for loss of interest/pleasure and somatic symptoms, with only the fornix associated with dysphoric mood and somatic symptoms severity. This suggests that different pathophysiology may underlie depression symptoms and by using symptoms subscales for depression, a different trend between white matter microstructure and symptom severity may be found.

To this end, we used subscales to measure depression symptomatology based off a confirmatory factor analysis of BDI-II in a PD population: 1) dysphoric mood, encompassing sadness and negative thoughts about self, 2) loss of interest/pleasure suggesting apathy component of depression, and 3) somatic symptoms representing physical complaints [19]. Using subscales to break down the symptoms of depression may help disentangle this complex syndrome, allowing for further understanding of the structural pathophysiology. Further, symptom-based findings may help understand certain phenotypes of depression and ultimately improve treatment with targeted strategies.

There are several limitations to this study. Like many other DTI studies, our cross-sectional analysis has a limited sample size. The small sample size limits the power of the study while increasing the possibility of type II error. Our study population was sourced from a cohort undergoing surgical planning for DBS that may limit the generalizability. Further, due to surgeon preference, most patients exhibiting depression symptoms were mildly depressed and therefore do not represent the full spectrum of depression. A larger cohort study using a similar standardized depression assessment tool and subscales is needed to help better assess the structural changes associated with depression symptomatology across the severity spectrum. Despite the statistical significance, the correlation between the left SCC-mPFC structural connectivity and dysphoric mood is limited by the low R^2, suggesting additional variables may aid in further explaining the variation seen in the DTI measures. Additional studies must control for potential confounding by PD symptom duration, and antidepressant medication use/status, which may impact structural connectivity. Regarding DTI measures, here we used an atlas-based approach and probabilistic tractography. Although commonly used in the literature, the atlas-based approach for our ROI-analysis has intrinsic limitations as it does not account for all inter-subject anatomic variability.

Nonetheless, this study can provide initial insight into the hypothesis that there are distinct DTI correlates of depression symptom subcategories. Strengths of this study include the quality of our dataset in providing comprehensive PD and psychological assessments. Further, the use of probabilistic tractography provides patient-specific targets and advantages over deterministic methods, which assumes fiber orientation at the voxel level. Future studies are needed with larger sample sizes to disentangle depression symptoms and their

neural correlates, as well as to investigate whether clinical symptom biomarkers may guide depression treatment selection in PD.

5. Conclusion

Neuroimaging studies have shed light on subtypes of MDD, important in treatment selection and predicting response. This study demonstrates that aberrant SCC structural connectivity, a neural network implicated in MDD, may underlie the pathophysiology of dysphoric mood in PD. We also find that FA is positively correlated with dysphoric mood, loss of interest/pleasure, and somatic symptom severity in disparate ROIs. Our findings provide insight to the pathophysiology of comorbid depression symptomatology in PD.

Acknowledgements:

We thank Dr. Patricia Walshaw for her assistance in providing the Beck Depression Inventory data.

Funding statement:

Research reported in this publication was supported by the National Institute Of Neurological Disorders and Stroke of the National Institutes of Health under Award Number R01NS097782. The content is solely the responsibility of the authors and does not necessarily represent the official views of the National Institutes of Health.

Data availability statement:

The data that support the findings of this study are available from the corresponding author upon reasonable request and subject to IRB approval.

References

[1]. Marsh L, 2013. Depression and Parkinson's Disease: Current Knowledge. Curr Neurol Neurosci Rep 13, 409. 10.1007/s11910-013-0409-5 [PubMed: 24190780]

[2]. Huang P, Xu X, Gu Q, Xuan M, Yu X, Luo W, Zhang M, 2014. Disrupted white matter integrity in depressed versus non-depressed Parkinson's disease patients: A tract-based spatial statistics study. Journal of the Neurological Sciences 346, 145–148. 10.1016/j.jns.2014.08.011 [PubMed: 25194633]

[3]. Matsui H, Nishinaka K, Oda M, Niikawa H, Komatsu K, Kubori T, Udaka F, 2006b. Depression in Parkinson's disease. J Neurol 254, 1170. 10.1007/s00415-006-0236-6 [PubMed: 17710361]

[4]. Li W, Liu J, Skidmore F, Liu Y, Tian J, Li K, 2010. White Matter Microstructure Changes in the Thalamus in Parkinson Disease with Depression: A Diffusion Tensor MR Imaging Study. American Journal of Neuroradiology 31, 1861–1866. 10.3174/ajnr.A2195 [PubMed: 20705702]

[5]. Jones DK, Knösche TR, Turner R, 2013. White matter integrity, fiber count, and other fallacies: The do's and don'ts of diffusion MRI. NeuroImage 73, 239–254. 10.1016/j.neuroimage.2012.06.081 [PubMed: 22846632]

[6]. Atkinson-Clement C, Pinto S, Eusebio A, Coulon O, 2017. Diffusion tensor imaging in Parkinson's disease: Review and meta-analysis. NeuroImage: Clinical 16, 98–110. 10.1016/j.nicl.2017.07.011

[7]. Jiang J, Zhao Y-J, Hu X-Y, Du M-Y, Chen Z-Q, Wu M, Li K-M, Zhu H-Y, Kumar P, Gong Q-Y, 2017. Microstructural brain abnormalities in medication-free patients with major depressive disorder: a systematic review and meta-analysis of diffusion tensor imaging. J Psychiatry Neurosci 42, 150–163. 10.1503/jpn.150341 [PubMed: 27780031]

[8]. Drevets WC, Savitz J, Trimble M, 2008. The Subgenual Anterior Cingulate Cortex in Mood Disorders. CNS Spectr 13, 663–681. [PubMed: 18704022]

[9]. Connolly CG, Wu J, Ho TC, Hoeft F, Wolkowitz O, Eisendrath S, Frank G, Hendren R, Max JE, Paulus MP, Tapert SF, Banerjee D, Simmons AN, Yang TT, 2013. Resting-State Functional Connectivity of Subgenual Anterior Cingulate Cortex in Depressed Adolescents. Biol Psychiatry 74, 898–907. 10.1016/j.biopsych.2013.05.036 [PubMed: 23910949]

[10]. Tsolaki E, Narr KL, Espinoza R, Wade B, Hellemann G, Kubicki A, Vasavada M, Njau S, Pouratian N, 2020. Subcallosal Cingulate Structural Connectivity Differs in Responders and Nonresponders to Electroconvulsive Therapy. Biological Psychiatry: Cognitive Neuroscience and Neuroimaging S2451902220301348. 10.1016/j.bpsc.2020.05.010

[11]. Lujan JL, Chaturvedi A, Choi KS, Holtzheimer PE, Gross RE, Mayberg HS, McIntyre CC, 2013. Tractography-activation models applied to subcallosal cingulate deep brain stimulation. Brain Stimul 6, 737–739. 10.1016/j.brs.2013.03.008 [PubMed: 23602025]

[12]. Tsolaki E, Espinoza R, Pouratian N, 2017. Using probabilistic tractography to target the subcallosal cingulate cortex in patients with treatment resistant depression. Psychiatry Research: Neuroimaging 261, 72–74. 10.1016/j.pscychresns.2017.01.006 [PubMed: 28142056]

[13]. de Schipper LJ, Hafkemeijer A, Bouts MJRJ, van der Grond J, Marinus J, Henselmans JML, van Hilten JJ, 2019. Age- and disease-related cerebral white matter changes in patients with Parkinson's disease. Neurobiology of Aging 80, 203–209. 10.1016/j.neurobiolaging.2019.05.004 [PubMed: 31207552]

[14]. Zheng Z, Shemmassian S, Wijekoon C, Kim W, Bookheimer SY, Pouratian N, 2014. DTI correlates of distinct cognitive impairments in Parkinson's disease. Hum Brain Mapp 35, 1325–1333. 10.1002/hbm.22256 [PubMed: 23417856]

[15]. Surdhar I, Gee M, Bouchard T, Coupland N, Malykhin N, Camicioli R, 2012. Intact limbic-prefrontal connections and reduced amygdala volumes in Parkinson's disease with mild depressive symptoms. Parkinsonism & Related Disorders 18, 809–813. 10.1016/j.parkreldis.2012.03.008 [PubMed: 22652466]

[16]. van Velzen LS, Kelly S, Isaev D, Aleman A, Aftanas LI, Bauer J, Baune BT, Brak IV, Carballedo A, Connolly CG, Couvy-Duchesne B, Cullen KR, Danilenko KV, Dannlowski U, Enneking V, Filimonova E, Förster K, Frodl T, Gotlib IH, Groenewold NA, Grotegerd D, Harris MA, Hatton SN, Hawkins EL, Hickie IB, Ho TC, Jansen A, Kircher T, Klimes-Dougan B, Kochunov P, Krug A, Lagopoulos J, Lee R, Lett TA, Li M, MacMaster FP, Martin NG, McIntosh AM, McLellan Q, Meinert S, Nenadić I, Osipov E, Penninx BWJH, Portella MJ, Repple J, Roos A, Sacchet MD, Sämann PG, Schnell K, Shen X, Sim K, Stein DJ, van Tol M-J, Tomyshev AS, Tozzi L, Veer IM, Vermeiren R, Vives-Gilabert Y, Walter H, Walter M, van der Wee NJA, van der Werff SJA, Schreiner MW, Whalley HC, Wright MJ, Yang TT, Zhu A, Veltman DJ, Thompson PM, Jahanshad N, Schmaal L, 2020. White matter disturbances in major depressive disorder: a coordinated analysis across 20 international cohorts in the ENIGMA MDD working group. Mol Psychiatry 25, 1511–1525. 10.1038/s41380-019-0477-2 [PubMed: 31471575]

[17]. Drysdale AT, Grosenick L, Downar J, Dunlop K, Mansouri F, Meng Y, Fetcho RN, Zebley B, Oathes DJ, Etkin A, Schatzberg AF, Sudheimer K, Keller J, Mayberg HS, Gunning FM, Alexopoulos GS, Fox MD, Pascual-Leone A, Voss HU, Casey BJ, Dubin MJ, Liston C, 2017. Resting-state connectivity biomarkers define neurophysiological subtypes of depression. Nature Medicine 23, 28–38. 10.1038/nm.4246

[18]. Dunlop BW, Rajendra JK, Craighead WE, Kelley ME, McGrath CL, Choi KS, Kinkead B, Nemeroff CB, Mayberg HS, 2017. Functional Connectivity of the Subcallosal Cingulate Cortex Identifies Differential Outcomes to Treatment with Cognitive Behavior Therapy or Antidepressant Medication for Major Depressive Disorder. Am J Psychiatry 174, 533–545. 10.1176/appi.ajp.2016.16050518 [PubMed: 28335622]

[19]. Kirsch-Darrow L, Marsiske M, Okun MS, Bauer R, Bowers D, 2011. Apathy and Depression: Separate Factors in Parkinson's Disease. J Int Neuropsychol Soc 17, 1058–1066. 10.1017/S1355617711001068 [PubMed: 22040900]

[20]. Smith SM, Jenkinson M, Woolrich MW, Beckmann CF, Behrens TEJ, Johansen-Berg H, Bannister PR, De Luca M, Drobnjak I, Flitney DE, Niazy RK, Saunders J, Vickers J, Zhang Y, De Stefano N, Brady JM, Matthews PM, 2004. Advances in functional and structural MR image analysis and implementation as FSL. Neuroimage 23 Suppl 1, S208–219. 10.1016/j.neuroimage.2004.07.051 [PubMed: 15501092]

[21]. Behrens TEJ, Woolrich MW, Jenkinson M, Johansen-Berg H, Nunes RG, Clare S, Matthews PM, Brady JM, Smith SM, 2003. Characterization and Propagation of Uncertainty in Diffusion-Weighted MR Imaging. Magnetic Resonance in Medicine 50, 1077–1088. 10.1002/mrm.10609 [PubMed: 14587019]

[22]. Behrens TEJ, Berg HJ, Jbabdi S, Rushworth MFS, Woolrich MW, 2007. Probabilistic diffusion tractography with multiple fibre orientations: What can we gain? NeuroImage 34, 144–155. 10.1016/j.neuroimage.2006.09.018 [PubMed: 17070705]

[23]. Smith SM, Jenkinson M, Johansen-Berg H, Rueckert D, Nichols TE, Mackay CE, Watkins KE, Ciccarelli O, Cader MZ, Matthews PM, Behrens TEJ, 2006. Tract-based spatial statistics: voxelwise analysis of multi-subject diffusion data. Neuroimage 31, 1487–1505. 10.1016/j.neuroimage.2006.02.024 [PubMed: 16624579]

[24]. Mori S, Oishi K, Jiang H, Jiang L, Li X, Akhter K, Hua K, Faria AV, Mahmood A, Woods R, Toga A, Pike B, Neto PR, Evans A, Zhang J, Huang H, Miller MI, Zijl P. van, Mazziotta J, 2008. Stereotaxic White Matter Atlas Based on Diffusion Tensor Imaging in an ICBM Template. Neuroimage 40, 570–582. 10.1016/j.neuroimage.2007.12.035 [PubMed: 18255316]

[25]. Koenigs M, Grafman J, 2009. The functional neuroanatomy of depression: Distinct roles for ventromedial and dorsolateral prefrontal cortex. Behavioural Brain Research 201, 239–243. 10.1016/j.bbr.2009.03.004 [PubMed: 19428640]

[26]. Koenigs M, Huey ED, Calamia M, Raymont V, Tranel D, Grafman J, 2008. Distinct Regions of Prefrontal Cortex Mediate Resistance and Vulnerability to Depression. J Neurosci 28, 12341–12348. 10.1523/JNEUROSCI.2324-08.2008 [PubMed: 19020027]

[27]. Matsui H, Nishinaka K, Oda M, Komatsu K, Kubori T, Udaka F, 2006a. Minor depression and brain perfusion images in Parkinson's disease. Mov Disord 21, 1169–1174. 10.1002/mds.20923 [PubMed: 16685687]

[28]. Luo C, Chen Q, Song W, Chen K, Guo X, Yang J, Huang X, Gong Q, Shang H-F, 2014. Resting-state fMRI study on drug-naive patients with Parkinson's disease and with depression. J Neurol Neurosurg Psychiatry 85, 675–683. 10.1136/jnnp-2013-306237 [PubMed: 24227759]

[29]. Cardoso EF, Fregni F, Martins Maia F, Boggio PS, Luis Myczkowski M, Coracini K, Lopes Vieira A, Melo LM, Sato JR, Antonio Marcolin M, Rigonatti SP, Cruz AC, Reis Barbosa E, Amaro E, 2008. rTMS treatment for depression in Parkinson's disease increases BOLD responses in the left prefrontal cortex. Int J Neuropsychopharmacol 11, 173–183. 10.1017/S1461145707007961 [PubMed: 17708780]

[30]. Blood AJ, Iosifescu DV, Makris N, Perlis RH, Kennedy DN, Dougherty DD, Kim BW, Lee MJ, Wu S, Lee S, Calhoun J, Hodge SM, Fava M, Rosen BR, Smoller JW, Gasic GP, Breiter HC, 2010. Microstructural Abnormalities in Subcortical Reward Circuitry of Subjects with Major Depressive Disorder. PLoS One 5. 10.1371/journal.pone.0013945

Key Points:

- Left SCC-mPFC connectivity is correlated with dysphoric mood symptoms in PD
- Distinct white matter tracts underlie dysphoric mood, loss of interest, and somatic symptoms
- Abnormal SCC connectivity is implicated in both MDD and depressive symptoms in PD

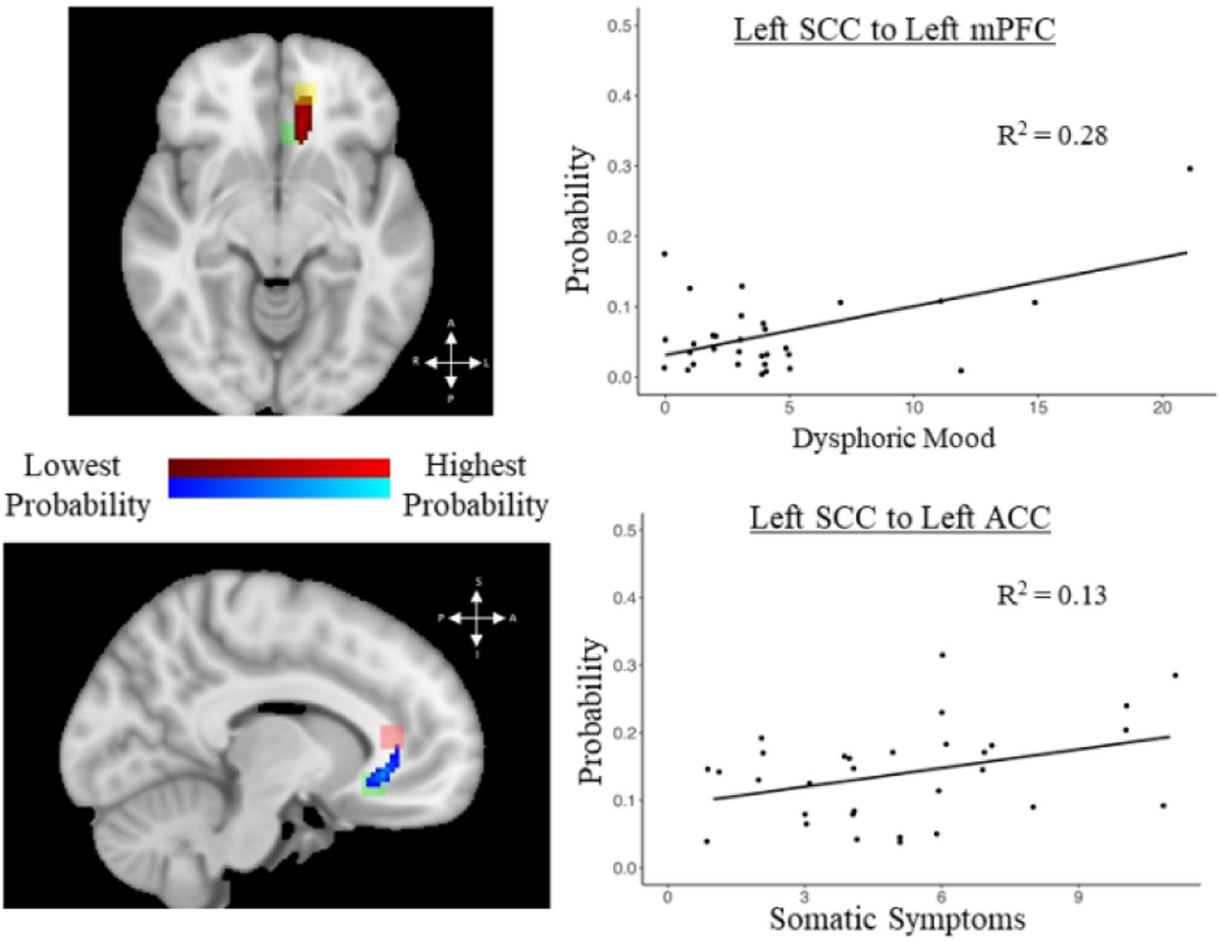

Figure 1.
Mean DTI measures

A) Boxplot of probability of connectivity from right and left SCC seeds to ROI targets: ipsilateral ACC, bilateral mPFC, ipsilateral UCF, and ipsilateral Vst. B) Boxplot of FA in the 48 JHU ROIs referenced in Table 1. Lower and upper boundaries of box correspond to the first and third quartiles; whiskers extend 1.5 times the inter-quartile range in both directions. Outlying points are plotted individually.

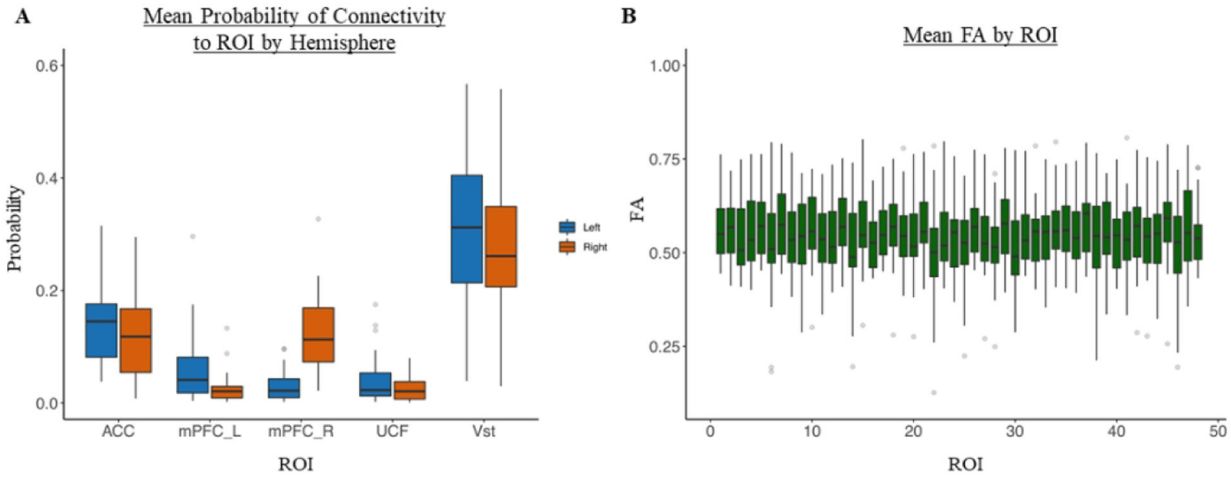

Figure 2.

Probability of connectivity correlations and depressive symptomatology

Left panel depicts group averaged left SCC-mPFC (red) and left SCC-ACC (blue) tracts overlaid on top of a standard brain, with a green box to delineate the SCC seed, yellow the mPFC mask, and pink the ACC. The right panel shows a scatter plot of left SCC-mPFC and dysphoric mood and of left SCC-ACC and somatic symptoms. Probability of connectivity positively correlated with symptom severity. A=anterior, P=posterior, S=superior, I=inferior.

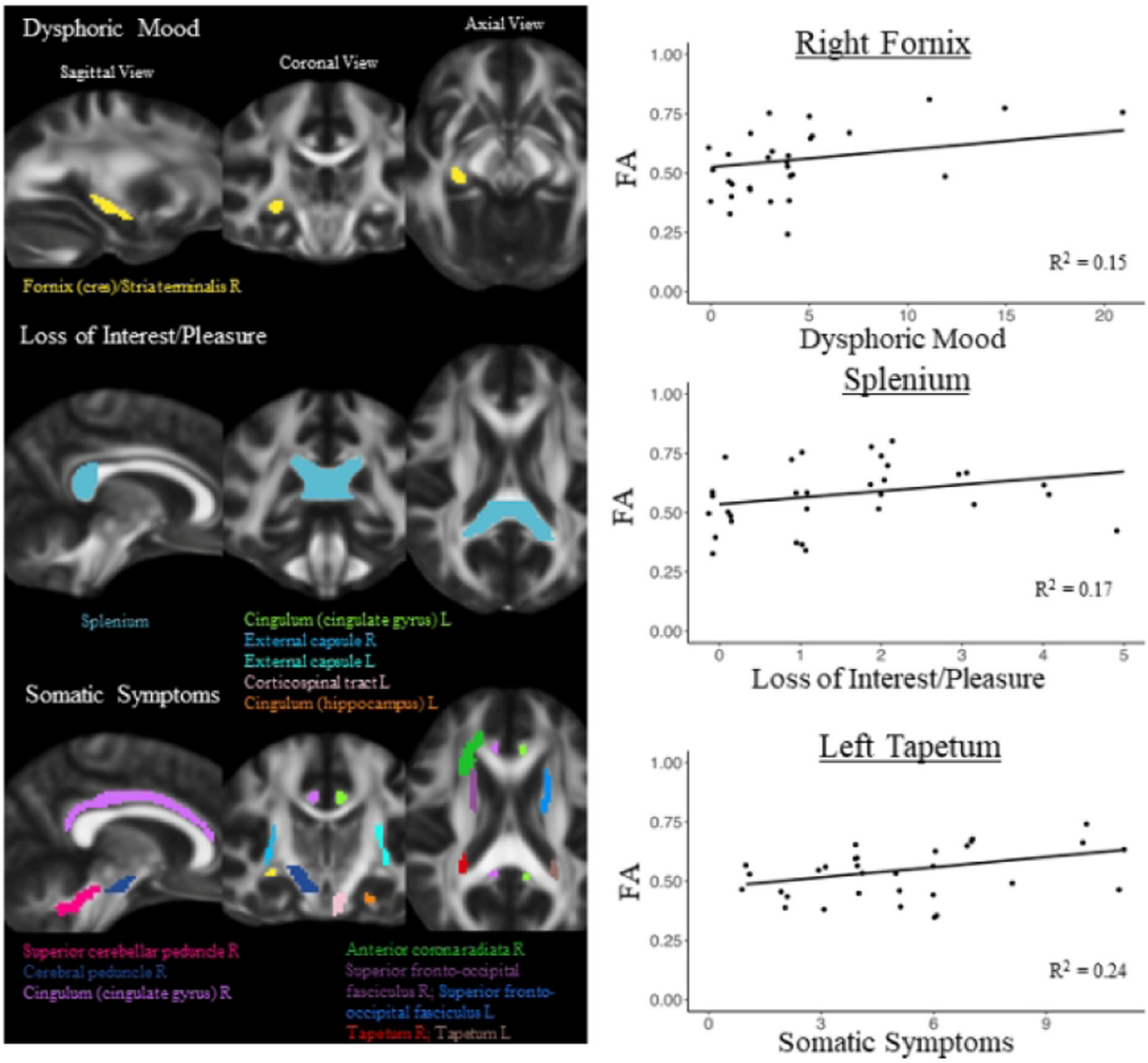

Figure 3.

ROI-based correlations and depressive symptomatology

Left panel depicts significant ROIs, after controlling for age and sex, overlaid on top of a standard brain for each depressive symptom: dysphoric mood, loss of interest/pleasure, and somatic symptoms. The right panel shows a scatter plot between significant ROI and depressive symptom. For somatic symptoms, the ROI with the lowest *p*-value is displayed. FA positively correlates with symptom severity.

Table 1.

JHU DTI-based white-matter atlas 48 ROI labels

Label	ROI
1	Middle cerebellar peduncle
2	Pontine crossing tract †
3	Genu of corpus callosum
4	Body of corpus callosum
5	Splenium of corpus callosum
6	Fornix (column and body of fornix)
7	Corticospinal tract R
8	Corticospinal tract L
9	Medial lemniscus R
10	Medial lemniscus L
11	Inferior cerebellar peduncle R
12	Inferior cerebellar peduncle L
13	Superior cerebellar peduncle R
14	Superior cerebellar peduncle L
15	Cerebral peduncle R
16	Cerebral peduncle L
17	Anterior limb of internal capsule R †
18	Anterior limb of internal capsule L
19	Posterior limb of internal capsule R
20	Posterior limb of internal capsule L
21	Retrolenticular part of internal capsule R
22	Retrolenticular part of internal capsule L
23	Anterior corona radiata R
24	Anterior corona radiata L
25	Superior corona radiata R
26	Superior corona radiata L
27	Posterior corona radiata R
28	Posterior corona radiata L
29	Posterior thalamic radiation (include optic radiation) R
30	Posterior thalamic radiation (include optic radiation) L
31	Sagittal stratum (include inferior longitudinal fasciculus and inferior fronto-occipital fasciculus) R
32	Sagittal stratum (include inferior longitudinal fasciculus and inferior fronto-occipital fasciculus) L
33	External capsule R
34	External capsule L
35	Cingulum (cingulate gyrus) R
36	Cingulum (cingulate gyrus) L

Label	ROI
37	Cingulum (hippocampus) R
38	Cingulum (hippocampus) L
39	Fornix (cres) / Stria terminalis R†
40	Fornix (cres) / Stria terminalis L
41	Superior longitudinal fasciculus R
42	Superior longitudinal fasciculus L
43	Superior fronto-occipital fasciculus R
44	Superior fronto-occipital fasciculus L
45	Uncinate fasciculus R
46	Uncinate fasciculus L
47	Tapetum R
48	Tapetum L

†Signifies missing FA value for one subject ($n = 30$)

Table 2.

Participant demographics and disease characteristics

	n (%) or mean (SD)
n	31
Male	24 (77.4%)
Female	7 (22.6%)
Age	64.5 (5.80)
Levodopa Equivalent	1126.33 (613.46)
UPDRS Score (in “off” state)[†]	35.11 (14.09)
Disease Duration, years	8.48 (3.38)
Depressive Symptomatology	
Dysphoric Mood	4.35 (0.830)
Loss of Interest/Pleasure	1.48 (0.245)
Somatic Symptoms	5.10 (0.509)

[†]Missing data for three participants (n=28)

Table 3.

Sensitivity analysis correlations, after controlling for age, sex, and UPDRS

A. Probabilistic tractography				
BDI-II Factor	**SCC Tract**	**Effect Estimate (se)**	***p*-value**	**Adjusted *p*-value**
Dysphoric mood	L SCC to L mPFC	0.0077 (0.0023)	0.003	0.015
B. ROI-based analysis				
BDI-II Factor	**ROI**	**Effect Estimate (se)**	***p*-value**	**Adjusted *p*-value**
Somatic	External capsule L	0.0123 (0.0057)	0.043	0.414
	Cingulum (cingulate gyrus) R	0.0130 (0.0055)	0.028	0.648
	Superior fronto-occipital fasciculus L	0.0128 (0.0059)	0.040	0.484
	Tapetum R	0.0151 (0.0064)	0.027	0.648
	Tapetum L	0.0131 (0.0050)	0.016	0.757

Multivariable model including age and sex underwent sensitivity analysis by including UPDRS (Unified Parkinson's Disease Rating Scale) in the model to control for motor function when examining the association of the SCC tracts and/or ROIs with depression symptomatology.

Table 4.

ROI-based correlations of FA and depressive symptoms, controlling for age and sex

BDI-II Factor	ROI	Multiple Regression	
		Effect Estimate (se)	p- value
Dysphoric mood	Fornix (cres) / Stria terminalis R	0.0070 (0.0032)	0.037
Loss of interest/pleasure	Splenium of corpus callosum	0.0262 (0.0126)	0.048
Somatic	Corticospinal tract L	0.0121 (0.0056)	0.041
	Superior cerebellar peduncle R	0.0122 (0.0051)	0.024
	Cerebral peduncle R	0.0140 (0.0063)	0.034
	Anterior corona radiata R	0.0167 (0.0068)	0.021
	External capsule R	0.0137 (0.0052)	0.014
	External capsule L	0.0139 (0.0054)	0.015
	Cingulum (cingulate gyrus) R	0.0150 (0.0052)	0.008
	Cingulum (cingulate gyrus) L	0.0133 (0.0055)	0.024
	Cingulum (hippocampus) L	0.0193 (0.0082)	0.026
	Fornix (cres) / Stria terminalis R	0.0124 (0.0052)	0.024
	Superior fronto-occipital fasciculus R	0.0140 (0.0059)	0.026
	Superior fronto-occipital fasciculus L	0.0158 (0.0056)	0.009
	Tapetum R	0.0174 (0.0059)	0.006
	Tapetum L	0.0150 (0.0046)	0.003

The subcallosal cingulate cortex (SCC) and its connections have been implicated in the pathophysiology of major depressive disorder (MDD). We used diffusion tensor imaging to examine the MDD-related structural abnormalities underlying depressive symptoms in PD (n=31). SCC (green box) and medial prefrontal cortex (yellow box) connectivity (group averaged red tract) in the left hemisphere was positively correlated with severity of dysphoric mood symptoms, suggesting abnormal SCC connectivity underlies depressive symptoms in both PD and MDD, particularly when depression in PD is dominated by dysphoric mood.